Attenuating homologous recombination stimulates an AID-induced antileukemic effect

Kristin R. Lamont,[1] Muneer G. Hasham,[1] Nina M. Donghia,[1] Jane Branca,[1] Margaret Chavaree,[2] Betsy Chase,[3] Anne Breggia,[4] Jacquelyn Hedlund,[3] Ivette Emery,[4] Francesca Cavallo,[5] Maria Jasin,[5] Jens Rüter,[2] and Kevin D. Mills[1]

[1]The Jackson Laboratory, Bar Harbor, ME 04609
[2]CancerCare of Maine, Eastern Maine Medical Center, Brewer, ME 04412
[3]Maine Center for Cancer Medicine, Scarborough, ME 04074
[4]Maine Medical Center Research Institute, Scarborough, ME 04074
[5]Memorial Sloan-Kettering Cancer Center, New York, NY 10065

Activation-induced cytidine deaminase (AID) is critical in normal B cells to initiate somatic hypermutation and immunoglobulin class switch recombination. Accumulating evidence suggests that AID is also prooncogenic, inducing cancer-promoting mutations or chromosome rearrangements. In this context, we find that AID is expressed in >40% of primary human chronic lymphocytic leukemia (CLL) cases, consistent with other reports. Using a combination of human B lymphoid leukemia cells and mouse models, we now show that AID expression can be harnessed for antileukemic effect, after inhibition of the RAD51 homologous recombination (HR) factor with 4,4′-diisothiocyanatostilbene-2-2′-disulfonic acid (DIDS). As a proof of principle, we show that DIDS treatment inhibits repair of AID-initiated DNA breaks, induces apoptosis, and promotes cytotoxicity preferentially in AID-expressing human CLL. This reveals a novel antineoplastic role of AID that can be triggered by inhibition of HR, suggesting a potential new paradigm to treat AID-expressing tumors. Given the growing list of tumor types with aberrant AID expression, this novel therapeutic approach has potential to impact a significant patient population.

CORRESPONDENCE
Kevin D. Mills:
Kevin.Mills@jax.org

Abbreviations used: AID, activation-induced cytidine deaminase; CLL, chronic lymphocytic leukemia; CSR, class switch recombination; DIDS, 4,4′-diisothiocyanatostilbene-2-2′-disulfonic acid; DSB, double-strand break; GC, germinal center; HR, homologous recombination; IR, ionizing radiation; mES cell, mouse embryonic stem cell; NLS, nuclear localization sequence; qPCR, quantitative PCR; UNG, uracil-DNA glycosylase; WBC, white blood cell.

In normal B lymphocytes, antigenic stimulation induces expression of activation-induced cytidine deaminase (AID), which drives somatic hypermutation and Ig class switch recombination (CSR; Muramatsu et al., 2000; Chaudhuri et al., 2003; McBride et al., 2006). AID generates point mutations and initiates DNA double-strand breaks (DSBs) in Ig genes and at widespread locations throughout the genome (McBride et al., 2006; Robbiani et al., 2009; Staszewski et al., 2011). Although its expression is normally restricted to activated B cells, AID can also be inappropriately expressed in a range of different malignancies, including lymphoid and myeloid leukemias (Klemm et al., 2009; Robbiani et al., 2009; Hancer et al., 2011). Ectopic or constitutive expression of AID in neoplastic cells is thought to contribute to a tumor-promoting mutator phenotype because of its widespread and promiscuous mutational and DNA breakage

activities (Okazaki et al., 2003; Heintel et al., 2004; Pasqualucci et al., 2008; Klemm et al., 2009; Robbiani et al., 2009; Shinmura et al., 2011). Although the functional significance of AID expression in tumors is not yet fully understood, it appears to have prooncogenic activities relating to tumor initiation, progression, or acquisition of therapy resistance in some cancers (Kou et al., 2007; Klemm et al., 2009; Liu et al., 2011; Shimizu et al., 2012).

Chronic lymphocytic leukemia (CLL), small lymphocytic lymphoma, and other related lymphoproliferative disorders are chronic, usually incurable, B lymphoid cancers that are common in aged populations (Yee and O'Brien, 2006). CLL and other B cell malignancies are heterogeneous and clinically variable. Although many patients exhibit stable disease requiring only watchful

K.R. Lamont and M.G. Hasham contributed equally to this paper.

monitoring, others show aggressive disease, therapy resistance, and rapid deterioration (Vasconcelos et al., 2003). For CLL patients requiring treatment, current standard of care involves rigorous chemotherapy, usually with purine analogues like fludarabine, which can induce temporary remission but rarely achieves cure (Yee and O'Brien, 2006; Zent and Kay, 2011). Moreover, current chemotherapy regimens are physically taxing, especially in elderly patients, exacerbating side effects, contributing to adverse outcomes, and reducing compliance (Zent and Kay, 2011). In addition, some subsets of patients show poor responses to standard first line chemotherapies, especially purine analogues (Steurer et al., 2006). Finally, devastating and long-term side effects can occur even in patients showing a favorable response (Yee and O'Brien, 2006; Zent and Kay, 2011). For all these reasons, new treatment paradigms that selectively target underlying CLL mechanisms or disease-specific features are urgently needed.

In mammalian cells, homologous recombination (HR) is a critical DNA DSB repair pathway. RAD51 is a core HR factor that mediates DNA strand exchange to initiate the recombination reaction (Shinohara et al., 1992; Sung and Robberson, 1995; Daboussi et al., 2002). RAD51 participates in multiple subcomplexes, together with a host of paralogous proteins (RAD51B, RAD51C, RAD51D, XRCC2, and XRCC3) that collectively define the RAD51 protein family (Kawabata et al., 2005; Thacker, 2005; Suwaki et al., 2011). We previously showed that HR is required at multiple stages of normal B cell maturation (Caddle et al., 2008; Hasham et al., 2010, 2012). Ablation of the RAD51 paralogue, XRCC2, leads to early B cell developmental arrest associated with stalled or collapsed DNA replication forks (Deans et al., 2000, 2003; Sale et al., 2001; Caddle et al., 2008; Hasham et al., 2010, 2012). In mature B cells, attenuation of XRCC2 by knockout or knockdown prevents repair of AID-initiated genome-wide DSBs and results in AID-dependent B cell cytotoxicity (Hasham et al., 2010). These findings suggested to us the possibility that HR attenuation might similarly sensitize AID-expressing neoplastic B cells to AID-mediated cytotoxicity and thus might represent a novel therapeutic approach.

As a proof of principle, we focused on CLL, showing that AID can exert an antileukemic effect when HR is attenuated. We demonstrate that 4,4′-diisothiocyanatostilbene-2-2′-disulfonic acid (DIDS), an inhibitor of RAD51 complex formation, potentiates AID-dependent human leukemia cell cytotoxicity (Ishida et al., 2009). We find that AID is expressed in >40% of human primary CLL cases and that its expression may be linked with key clinical parameters such as age at diagnosis or likelihood of treatment. Significantly, we show that AID-expressing primary human CLL cells are acutely and selectively hypersensitized to DIDS, which inhibits the repair of AID-dependent DSBs and leads to CLL cell death. Collectively, our findings establish a new biological principle: endogenously expressed AID activity can be rendered antineoplastic by small molecule inhibition of HR. We now define a new therapeutic paradigm based on this synergistic toxicity principle, which is distinct from conventional chemotherapies.

This approach has the potential to induce tumor cell self-destruction while minimizing side effects in tissues lacking AID expression. Given the growing body of evidence for AID activity in a range of tumor types, including CLL and other hematologic malignancies, this therapeutic concept may be broadly applicable in a significant range of cancers.

RESULTS

DIDS inhibits RAD51 nuclear import and focus formation

To determine whether the AID-dependent cytotoxicity that we previously observed in primary mouse B cells (by genetic knockdown of HR factors) could be mimicked by small molecules, we performed a differential sensitivity screen for compounds to which $AID^{+/+}$ but not $AID^{-/-}$ B cells were selectively sensitive (Fig. 1, A and B). We screened a total of 470 compounds and identified DIDS as a candidate (Fig. 1 B). DIDS is a disulfonated trans-stilbene derivative that binds to RAD51 and inhibits its DNA binding and strand exchange activities (Ishida et al., 2009).

To confirm that DIDS inhibits RAD51-mediated DNA damage repair in B lymphocytes, we evaluated radiosensitivity in the CH12-F3 mouse B cell lymphoma cell line, with or without DIDS. CH12-F3 cells were cultured with 0, 50, 100, or 150 µM DIDS and exposed to either 0 or 2.5 Gy of ionizing radiation (IR; Fig. 2 A). 2 d after irradiation, viable cells were quantified for each condition. This analysis revealed DIDS dose–dependent radiosensitization, with irradiated cells exposed to
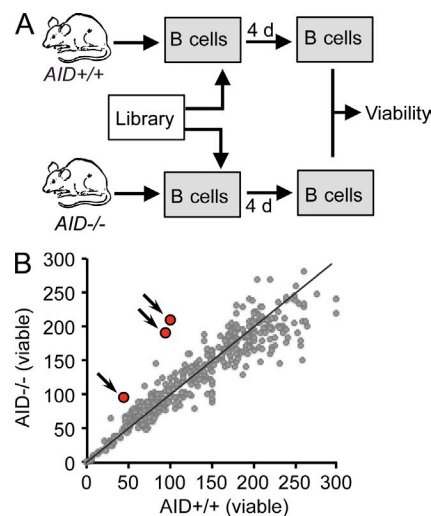

Figure 1. Compound screening for inhibitors of HR identifies DIDS as a candidate. (A) Schematic of compound screening for inhibitors of HR. In total, 470 compounds were screened from the NCI Diversity Set. (B) Differential plot showing compound screening data for $AID^{+/+}$ versus $AID^{-/-}$ cells. Viable cell counts for $AID^{-/-}$ (y axis) versus $AID^{+/+}$ (x axis) are plotted, with each data point representing an individual compound. Compounds to which $AID^{-/-}$ cells are more resistant than $AID^{+/+}$ cells deviate vertically above the diagonal and are considered "hits." Data points representing 150 µM DIDS are shown in red and denoted by arrows (three independent trials).

150 µM DIDS showing <40% viability relative to DIDS–naive cells (Fig. 2 A). This radiosensitization by DIDS is consistent with a DNA repair inhibitory activity.

To measure the extent of HR suppression by DIDS, we quantified HR activity using a GFP–based recombination reporter system in both human U2OS and mouse embryonic stem cells (mES cells; Fig. 2, B–D). In both reporter systems, cells harbor direct, nonfunctional repeats of the GFP (DR–GFP) in the genome (Moynahan et al., 2001; Nakanishi et al., 2005). A DSB introduced into one GFP repeat by the I-SceI endonuclease can be repaired from the second GFP gene, producing a functional GFP gene (Fig. 2 B). HR efficiency with this system can be sensitively measured by flow cytometry to detect GFP+ cells (Fig. 2 B). Treatment of either U2OS or mES

cells with DIDS reduced HR, consistent with an inhibition of RAD51 activity in vivo (Fig. 2, C and D).

To confirm that DIDS exposure disrupted RAD51, we measured irradiation–induced RAD51 focus formation with or without DIDS (Fig. 2, E–G). Splenic B cells were isolated from normal adult mice and cultured in the presence of either 0 or 150 µM DIDS. Cells were then subjected to 0 or 2.5 Gy of IR, allowed to recover for 1 d, and fixed for immunofluorescent imaging of RAD51. Baseline RAD51 staining in untreated, nonirradiated cells was dimly diffuse (Fig. 2, E–G). Nonirradiated cells treated with 150 µM DIDS showed diffuse RAD51 staining plus significant extranuclear accumulation in the cytoplasm. After exposure to 2.5 Gy of irradiation, cells without DIDS showed stereotypical punctate staining of
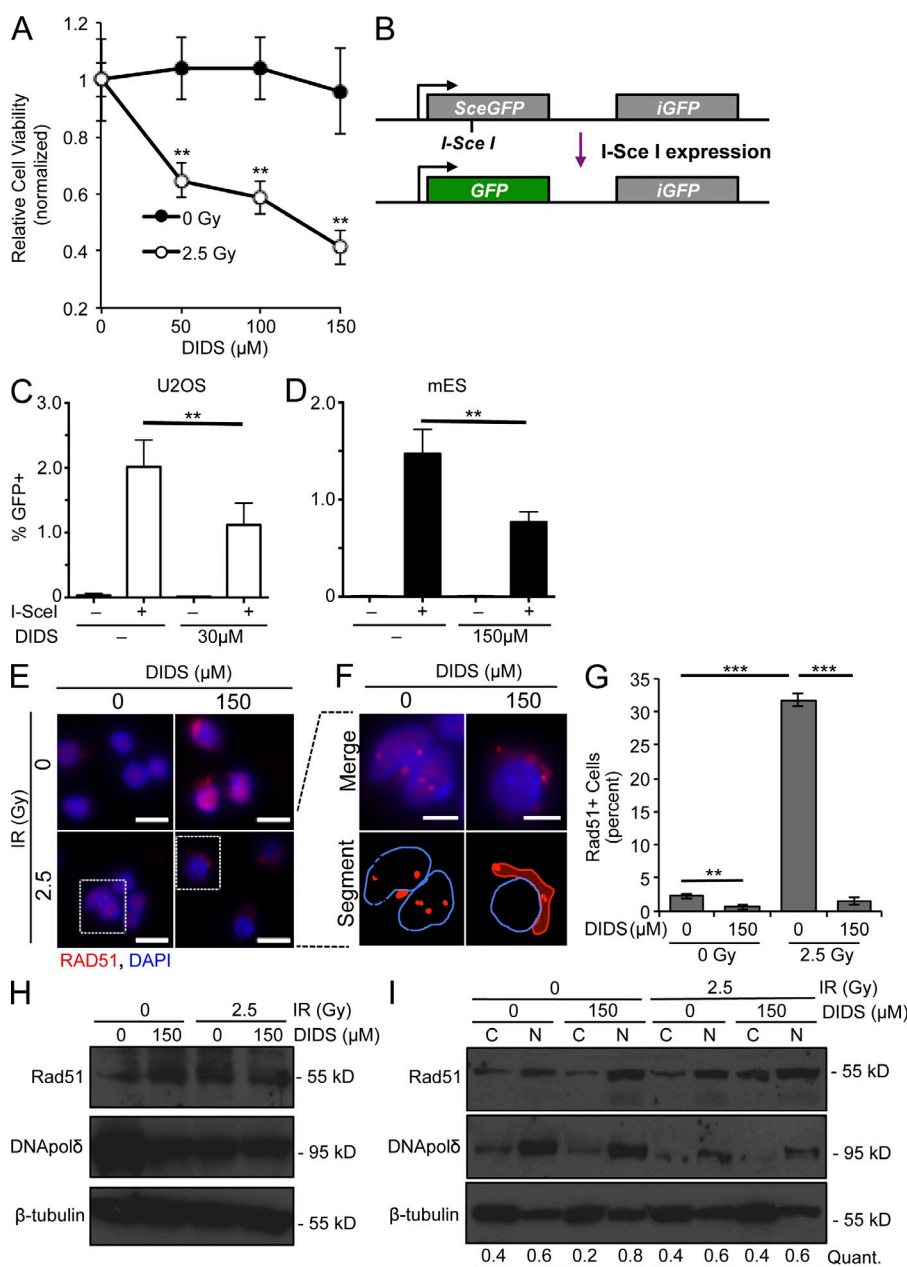

Figure 2. DIDS inhibits RAD51 complex formation and sensitizes cells to IR.
(A) Viability analysis of CH12-F3 cells 24 h after exposure to either 0 or 2.5 Gy IR in the presence of the indicated concentrations of DIDS. Data are normalized to the fraction of cells for each IR dose that received 0 µM DIDS; error bars represent the SEM for three independent experiments. (B) Schematic of construct used for DR-GFP assay. (C and D) Analysis of HR in U2OS (C) and mES (D) cell lines containing the DR-GFP reporter electroporated with an I-SceI or control expression vector in the presence or absence of 30 µM and 150 µM DIDS, respectively. Data are from four independent experiments; error bars represent 1 SD. Statistical analysis was performed using a paired two-tail Student's t test. (E) Immunofluorescence detection of RAD51 in primary mouse B cells 24 h after irradiation (0 or 2.5 Gy) with or without 150 µM DIDS. RAD51 staining is indicated in red, and nuclear DNA (DAPI stained) is shown in blue. (F) Magnification of cells in bottom panels of E. Manually segmented images (bottom) in which nuclear periphery and RAD51 localization in top images were drawn; blue outlines delineate nuclear periphery, and red outline indicates cytoplasmic RAD51 signal. Bars: (E) 10 µm; (F) 4.4 µm. (G) Quantification of cells that exhibit RAD51 signal in nucleus (RAD51+) from D and E. Error bars represent the SEM for three independent experiments. (H and I) Cell fractionation assay of primary mouse B cells irradiated and treated with DIDS as in E–G. Whole cell lysates (H) and cytoplasmic (C)/nuclear (N) fractions (I) were analyzed by Western blotting for RAD51, DNA polδ, and β-tubulin. Values below the panels on right represent the fraction of RAD51 in that compartment compared with RAD51 signal in C+N, determined by densitometry. Student's t test p-values: ***, $P < 0.001$; **, $P = 0.001-0.1$.
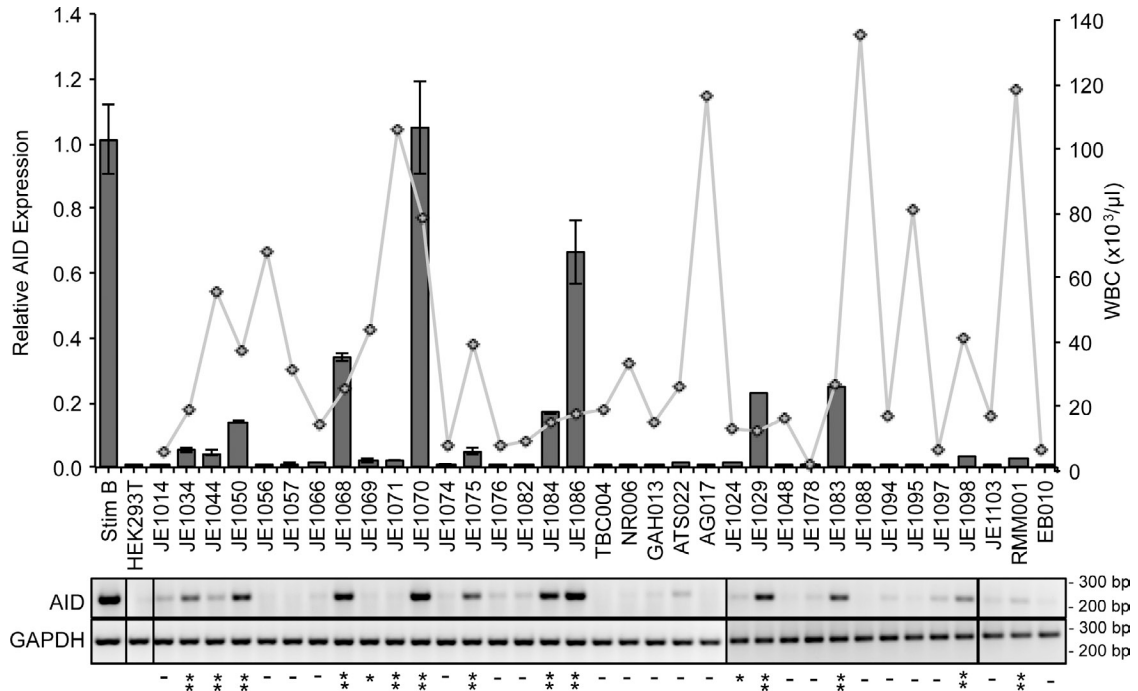
Figure 3. AID is expressed in a significant fraction of primary CLL tumor specimens. Total RNA was prepared from PBMCs from 74 patients diagnosed with CLL and used in real-time qPCR (top) and RT-PCR analysis (bottom) of AID expression. Only the data for 35 patient samples are shown. Water (H$_2$O) and embryonic kidney cells (HEK293T) cells were used as negative controls for template and AID expression, respectively, and human activated B lymphocytes (Stim B) were used as a positive control. GAPDH was used as a loading control. qPCR C$_T$ values for AID expression were normalized to GAPDH and then normalized to Stim B, whose expression was set at 1. Error bars represent the SEM of three independent analyses for each sample. Patient WBC values are also plotted, with axis on the right. Samples that do not express AID (within 3 SD of the negative control) are denoted by a dash (-); samples determined to express AID (between 3 and 5 SD of the negative control) are labeled with a single asterisk (*); strongly expressing samples (>5 SD of the negative control) are labeled with a double asterisk (**). Black lines indicate that intervening lanes were spliced out.

RAD51 foci in cell nuclei, indicating recruitment of RAD51 complexes to DSBs (Fig. 2, E–G). Approximately 30% of irradiated, DIDS-naive cells retained RAD51 foci 24 h after irradiation (Fig. 2 G). In contrast, irradiated B cells that were treated with 150 µM DIDS showed cytoplasmic accumulation of RAD51 and lacked the characteristic nuclear foci (Fig. 2, E–G). This finding was further supported by subcellular fractionation analysis to measure RAD51 nucleocytoplasmic partitioning. Cytoplasmic and nuclear protein fractions were prepared from irradiated (or untreated control) mouse B cells exposed to either 0 or 150 µM DIDS and analyzed by Western blotting for RAD51 protein. We observed increased RAD51 in the cytoplasmic fractions of irradiated cells that were treated with DIDS, consistent with immunofluorescence data showing defective nuclear localization (Fig. 2 H). Collectively, these data demonstrate a DSB repair inhibitory activity for DIDS in primary B cells associated with direct disruption of RAD51 complex formation.

AID expression is common in primary CLL cells

To test whether DIDS could, in principle, trigger an AID-dependent antitumor effect, as predicted, we focused our proof of principle experiments on human CLL, a B cell neoplasm which often expresses AID (Table S1; Palacios et al., 2010).

We designed an iterative research strategy combining analyses of human primary leukemia samples with mechanistic testing in genetically defined mouse models. Because mouse B lymphocytes represent the closest experimental counterpart to human primary CLL lymphocytes, this experimental design enabled us to measure the combined effects of AID plus DIDS in patient-derived clinical samples while concurrently testing molecular mechanisms using the mouse system. Comparative analysis of dose sensitivity showed primary human cells to be sensitive to DIDS at doses of 10–30 µM, whereas primary mouse B cells showed significant sensitivity at doses of 50–150 µM (see Figs. 4 A and 5 A; and not depicted). Although the basis for this difference is not known, it may relate to interspecies differences in expression or activity of HR factors.

To identify patient samples for analysis, primary PBMCs were collected from 74 CLL patients (Table S1). Quantitative PCR (qPCR) and RT-PCR analyses revealed detectable AID mRNA in 46% (34/74) of the CLLs analyzed, with high levels in 20% (15/74) of the cases (Fig. 3 and Table S1). Expression of AID did not correlate with circulating CLL burden in these patients, as represented by white blood cell (WBC) count (Fig. 3). We selected eight AID-expressing (AID$^+$) and eight AID-negative (AID$^-$) CLL samples for further analysis, matching

Table 1. CLLs used for in vitro assays

CLL ID#	AID expression	WBCs	% lymph	Sex	Age at diagnosis	Treatment
					yr	
JE1015[a]	−	20.4	58.1	M	86	none
JE1019[a,b,c]	−	102.5	95.8	M	76	none
JE1031[a]	−	32.6	80.7	F	47	none
JE1056[b,c]	−	68.1	91.1	M	70	none
JE1057[a]	−	31.3	81.3	F	64	none
JE1069[b,c]	−	44.1	91.7	F	74	none
JE1088[b,c]	−	135.4	93.5	M	67	none
JE1095[b,c]	−	80.7	90.0	M	81	none
JE1010[a]	+	43.6	83.2	F	51	none
JE1036[a]	+	22.6	65	M	63	none
JE1044[b,c]	+	55.3	93.7	F	57	i.v. Ig
JE1045[b,c]	+	17.1	68.7	M	62	fludarabine
JE1046[b,c]	+	47.8	89.5	M	79	none
JE1070[a,b,c]	+	78.3	91.0	M	53	chlorambucil
JE1075[a]	+	39.3	87.6	F	72	none
JE1098[b,c]	+	41.2	86.0	F	73	chlorambucil

[a]Used in in vitro viability assays (Fig. 4 A).
[b]Used in γ-H2AX immunofluorescence assays (Fig. 7, A–C; and Fig. 8).
[c]Used in AC3 immunofluorescence assays (Fig. 4, B and C).

as closely as possible all other available clinical parameters, including age at diagnosis, total WBC counts, and the percentage of circulating lymphocytes (Table 1).

DIDS triggers AID–dependent cytotoxicity in human malignant B cells

To test whether DIDS could trigger AID-dependent cytotoxicity in primary, patient-derived CLL cells, PBMCs from AID^+ and AID^- subsets were cultured for 8 d in the presence of 30 μM DIDS and assessed for cellular viability at 2-d intervals (Fig. 4 A). By 6 d in the presence of DIDS, AID^+ CLL specimens showed a roughly twofold greater reduction in viability than AID^- specimens (40% reduction in AID^+ versus a 20% reduction in AID^- cells; Fig. 4 A). Immunostaining of DIDS-treated CLL cells for activated caspase-3 ($AC3^+$), a marker of apoptosis, showed that DIDS-triggered cytotoxicity in AID^+ CLL cells was associated with apoptotic cell death.(Fig. 4, B and C).

DIDS–induced cytotoxicity in B cells is AID dependent

To directly and definitively assess the AID dependency, we measured DIDS-stimulated cytotoxicity in $AID^{+/+}$ versus $AID^{-/-}$ mouse B cells. Purified B cells were activated by α–CD40 plus IL-4, exposed to DIDS ranging from 0 to 150 μM, and analyzed for cell viability at 2-d intervals up to 6 d. B cell cultures from both $AID^{+/+}$ and $AID^{-/-}$ mice that were unactivated (α–CD40 only) remained viable in all doses of DIDS (not depicted). As with the CLL cells, we observed AID-dependent, dose-related cytotoxicity in mouse B cells (Fig. 5 A). There was no significant difference between 0 and 50 μM DIDS treatment in either $AID^{+/+}$ or $AID^{-/-}$ B cells. In contrast, 100 μM DIDS produced an intermediate effect, and 150 μM DIDS elicited a significant

reduction in cell viability, specifically in $AID^{+/+}$ B cells. Importantly, $AID^{-/-}$ B cell cultures survived all DIDS doses similarly to untreated controls, showing that activation-induced B cell death in the presence of DIDS is AID dependent (Fig. 5 A). We obtained similar results for the mouse B lymphoid leukemia cell line CH12-F3 (Fig. 5, B and C). To verify AID dependency in human leukemia cells, we measured DIDS sensitivity in the AID-expressing human acute lymphoblastic leukemia line CCRF-SB, with or without shRNA–mediated knockdown of AID (Fig. 6, A and B). After 5 d in culture with 150 μM DIDS, viability of CCRF-SB cells harboring a scrambled control shRNA showed ∼40% viability relative to vehicle-treated cells, whereas knockdown of AID by shRNA exhibited significantly enhanced resistance to DIDS (Fig. 6 B).

Ig CSR in normal B cells involves uracil–DNA glycosylase (UNG) activity, downstream of AID-initiated cytidine deamination (Zan and Casali, 2008). To test whether the AID-mediated antileukemic effect similarly involves UNG, and thus might reflect a CSR-like molecular mechanism, we tested DIDS sensitivity in WT versus UNG1-deficient ($Ung1^{-/-}$) mouse B cells. Whereas loss of AID renders B cells resistant to DIDS-triggered cytotoxicity, UNG1-deficient B cells were as sensitive to DIDS as WT controls (Fig. 6, C and D). This shows that the antileukemic effect triggered by HR inhibition is, at least partially, independent of UNG and likely reflects a molecular pathway that is distinct from the canonical CSR pathway.

DIDS inhibits repair of AID–initiated DSBs in malignant and nontransformed B cells

HR is required to repair DNA DSBs resulting from endogenous or exogenous insult (Moynahan and Jasin, 2010). To test
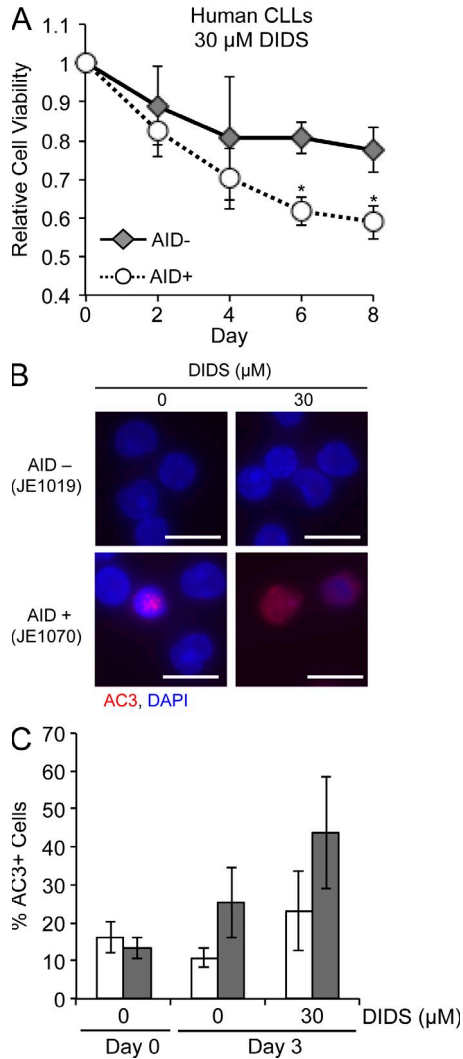
Figure 4. DIDS stimulates AID–dependent cytotoxicity in human CLL cells. (A) Viability of patient-derived CLL PBMCs cultured with 30 µM DIDS for up to 8 d. Viability was determined by counting of Trypan blue dye excluding cells via hemocytometer. DIDS-treated cells were normalized to untreated (0 µM DIDS) counterparts, and the plot represents the mean relative cell viability. Error bars represent the SEM for $n = 4$ tumors in each category. (B) Representative immunofluorescence microscopy images of AC3 staining in CD5^{+} CD19^{+} sorted CLL cells from an AID^{−} patient sample (JE1019) and an AID^{+} patient sample (JE1070). Cells were imaged on day 3 after treatment with or without 30 µM DIDS. Bars, 10 µm. (C) Percentage of AC3^{+} cells represented in B, counting ∼100 cells per treatment. Error bars represent the SEM for $n = 4$ and $n = 5$ tumors for AID[−] (open bars) and AID[+] (gray bars), respectively. Unpaired Student's t test p-value: *, P = 0.01–0.05.

whether DIDS–mediated cytotoxicity affects repair, we measured γ-H2AX foci formation, a known marker of DSBs (Rogakou et al., 1998), in human CLL and primary mouse B cells (Figs. 7 and 8). Untreated AID^{+} and AID^{−} purified CLL (CD5^{+} CD19^{+}) samples were indistinguishable, showing equivalent fractions with low (1–2 foci/nucleus), moderate (3–10 foci/nucleus), and high (>10 foci/nucleus) levels of unrepaired DSBs (Fig. 7, A–C). In contrast, exposure to 30 µM
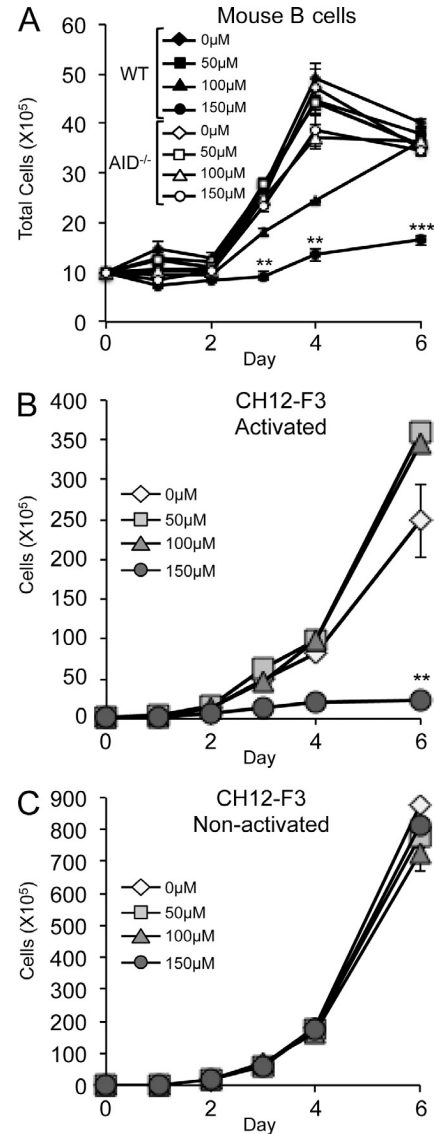

Figure 5. DIDS stimulates AID–dependent cytotoxicity in normal and malignant mouse B cells. (A) Measurement of cell proliferation of primary AID^{+/+} splenocytes, activated to induce CSR via α-CD40/IL-4 treatment on days 0 and 2, in the presence of the indicated concentrations of DIDS. Measurement of cell proliferation was determined by Trypan blue staining and counting of viable cells via hemocytometer. Data are represented as the mean cell count for each condition. (B and C) Proliferation of activated (B) or non-activated (C) CH12-F3 cells after treatment with the indicated concentrations of DIDS. CH12-F3 cells in B were activated on day 0 and restimulated on day 2 with α-CD40, IL-4, and TGF-β. CH12-F3 cells in C were only administered α-CD40 on days 0 and 2. Viability was determined by Trypan blue exclusion test. (A–C) Error bars represent the SEM for three independent experiments. Unpaired Student's t test p-values: ***, P < 0.001; **, P = 0.001–0.1.

DIDS induced a threefold increase in cells with moderate DNA damage (3–10 foci/nucleus) and a 6.5-fold increase in cells with high DNA damage (>10 foci/nucleus) in AID[+] samples relative to AID[−] samples (Fig. 7 C), notwithstanding patient to patient variability in response to DIDS treatment (Fig. 8). This experiment confirms that HR inhibition via DIDS
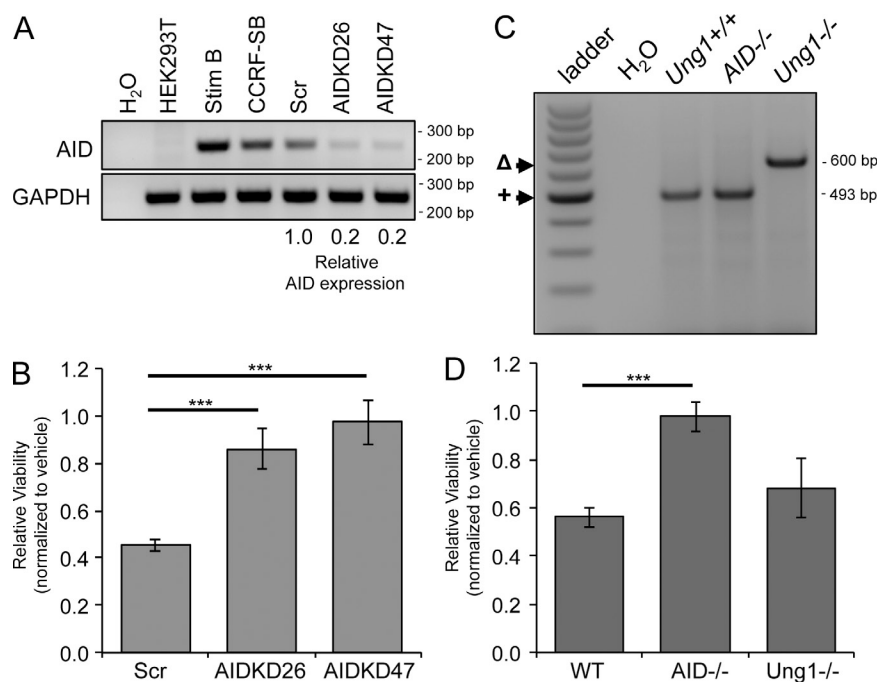
Figure 6. AID is required to induce DIDS cytotoxicity in malignant B cells. (A) RT-PCR analysis of AID expression 72 h after shRNA transduction in CCRF-SB cells. Water (H_2O) and RNA from human embryonic kidney cells (HEK293T) cells were used as negative controls for template and AID expression, respectively, and human activated B lymphocyte RNA (Stim B) was used as a positive control. GAPDH was used as a loading control. Values below images represent densitometry analysis and were normalized to GAPDH, and the expression of AID in Scr was set at 1. (B) Viability of shRNA-transduced CCRF-SB cells after treatment with 150 µM DIDS for 5 d. Viability was determined by Trypan blue staining and counting of cells via hemocytometer. Data are normalized to vehicle-treated (DMSO) cells in each transduction group. Error bars represent the SEM for $n = 6$ samples. (C) Genotyping reaction for $Ung1$ (UNG) knockdown from the spleen of the indicated mice. "+" denotes the expected PCR product size produced from the WT allele of Ung, whereas "Δ" denotes the expected size of the deleted Ung allele. (D) Viability assay of sorted B cells that were activated with α-CD40 and IL-4 and treated with either 150 µM DIDS or DMSO vehicle for 4 d. Data are normalized to DMSO-treated cells in each genotype. Error bars represent the SEM for $n = 6$ samples from each of two mice for WT and $AID^{-/-}$ and $n = 3$ samples for $Ung1^{-/-}$. Unpaired Student's t test p-values: ***, $P < 0.001$.

treatment leads to unrepaired DSBs that cause cytotoxicity in AID-expressing CLL cells.

To definitively test AID dependency, parallel assays were performed in primary mouse B cells from either $AID^{+/+}$ or $AID^{-/-}$ mice. B cell cultures were activated for 3 d with α-CD40 and IL-4 in the presence or absence of DIDS and analyzed for γ-H2AX foci. Confirming the data from primary human CLL cells, $AID^{+/+}$ B cell cultures harbored significantly more cells with a high level of unrepaired DSBs (>10 foci/nucleus) than the counterpart $AID^{-/-}$ control cultures (Fig. 7, D and E). Cell cycle analysis showed a negligible effect of DIDS on the cell cycle distribution of activated B lymphocytes from either $AID^{+/+}$ or $AID^{-/-}$ animals (not depicted). From these results, we conclude that DIDS inhibits the repair of AID-mediated DSBs, leading to accumulation of γ-H2AX foci at sites of unrepaired DNA breakage in AID-expressing cells.

In vivo DIDS treatment selectively targets AID-positive lymphocytes

To test whether DIDS could selectively induce cytotoxicity in AID-expressing cells in vivo, either $AID^{+/+}$ or $AID^{-/-}$ mice were administered 50 mg/kg DIDS at weekly intervals, immunized at weeks 1 and 4 with dinitrophenol-conjugated keyhole limpet hemocyanin (DNP-KLH) to stimulate lymphocyte activation, and analyzed after a total of 7 wk (Fig. 9 A). No animals in either the control or DIDS-treated groups showed overt signs of toxicity, relative to the untreated control

groups. After 5 wk, the $AID^{+/+}$ mice showed slightly greater weight gain than the $AID^{-/-}$ mice, but this effect was independent of DIDS exposure, affecting the 0-mg/kg control and 50-mg/kg experimental cohorts equally (Fig. 9 B). After the 7-wk trial window, tissues from treated and control animals were fixed, sectioned, and analyzed after hematoxylin and eosin (H&E) staining. Analysis of spleen sections revealed no gross anatomical defects or differences in germinal center (GC) architecture between untreated and DIDS-treated animals, as well as no differences between $AID^{+/+}$ mice and $AID^{-/-}$ controls (Fig. 9 C). These data suggest that DIDS, at least up to 50 mg/kg, does not induce significant toxicity or general defects in splenic physiology in either $AID^{+/+}$ or $AID^{-/-}$ mice. To determine whether DIDS induced a B cell–specific phenotype related to AID, we next analyzed bone marrow, spleen, and peripheral blood from DIDS-treated $AID^{+/+}$ versus $AID^{-/-}$ mice for the presence of B220^{+} CD19^{+} B cells by flow cytometry. We observed a small (25%) reduction in B220^{+} CD19^{+} B cells in the bone marrow of both 10 mg/kg– and 50 mg/kg–treated $AID^{+/+}$ mice, but no consistent differences in the percentages of splenic B cells in either $AID^{+/+}$ or $AID^{-/-}$ were observed (Fig. 9 D). In contrast, both 10 mg/kg and 50 mg/kg DIDS induced a significant (9–11-fold) reduction in circulating B lymphoid cells specifically in $AID^{+/+}$ but not $AID^{-/-}$ mice (Fig. 9 D). These data suggest that in vivo, systemic DIDS treatment selectively affected mature, post-GC B cells but had a negligible effect on early or pre-GC B cells. This is consistent with our
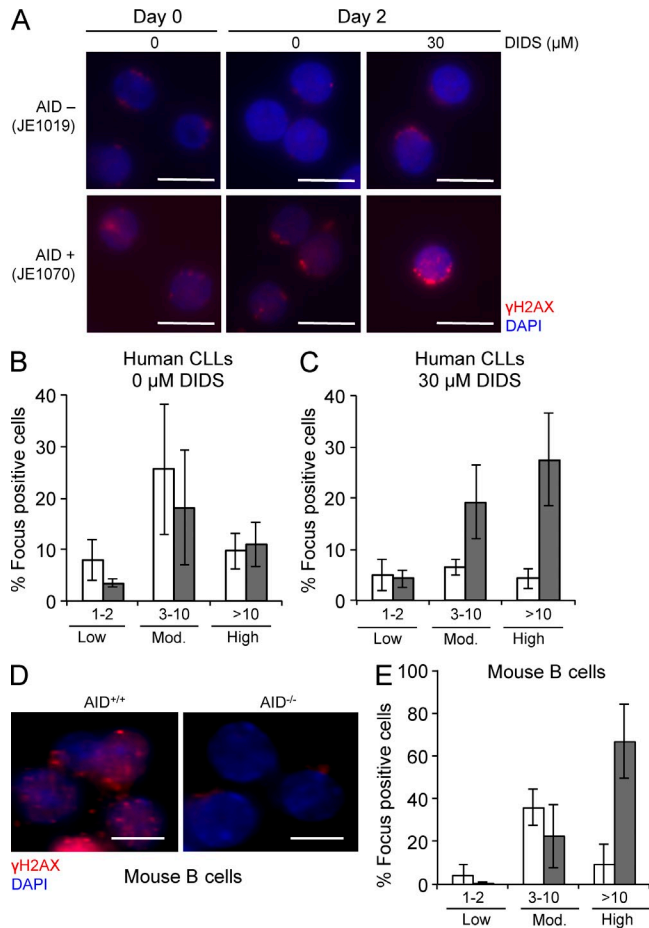
Figure 7. DIDS prevents repair of AID–induced DNA DSBs in malignant and nontransformed B cells. (A) Representative immunofluorescence images of phosphorylated γ-H2AX in purified CD5+ CD19+ CLL cells from an AID− (JE1019) and an AID+ (JE1070) patient sample. Cells were treated for 0–2 d with or without 30 µM DIDS. (B and C) Quantitation of foci observed in CLL cells after 2 d of culture in the absence (B) or presence (C) of 30 µM DIDS. Data were grouped into binds of cells with low (1–2 foci per nucleus), moderate (3–10 foci per nucleus), or high (>10 foci per nucleus) DNA damage. Error bars represent the SEM for $n = 4$ and $n = 5$ tumors for AID− (open bars) and AID+ (gray bars), respectively. (D) Representative immunofluorescence microscopy images of phosphorylated γ-H2AX foci in activated mouse splenic B cells after 3 d in the presence of 150 µM DIDS. (E) Percentage of *AID*+/+ (gray bars) or *AID*−/− (open bars) cells with low (1–2 foci per nucleus), moderate (3–10 foci per nucleus), or high (>10 foci per nucleus) DNA damage. Error bars represent the SEM for $n = 4$ (AID− CLLs), $n = 5$ (AID+ CLLs), and $n = 3$ (*AID*−/−, *AID*+/+ mouse B cells) experiments. Bars, 10 µm.

cell culture data demonstrating a synergistic cytotoxicity induced by the combined effects of AID and DIDS. Significantly, none of the DIDS-treated animals, in either the *AID*+/+ or *AID*−/− cohort, showed evidence of overt non–B cell toxicity. Collectively, these data clearly demonstrate that in vivo administration of DIDS specifically affects AID-expressing B cells. Also, at the concentrations tested, DIDS is well tolerated by mice and has negligible toxicity on other, non–AID-expressing, tissues.

DISCUSSION

Here we describe a potential new synthetic lethal therapeutic approach for the treatment of AID-expressing B cell malignancies: attenuation of RAD51-mediated HR to inhibit repair of endogenous AID-generated DSBs, culminating in cytotoxicity. This approach uses inherent recombinase activity, rather than systemically administered genotoxic agents, to induce cell-lethal genomic damage. As such, this strategy represents a special case of synthetic lethal therapy. We establish the proof of principle, showing that AID-expressing human CLL cells are hypersensitive to DIDS, a RAD51 inhibitor. Using a combination of primary patient-derived CLLs and genetic mouse models, we establish that DIDS treatment inhibits repair of AID-mediated DSBs in AID-expressing, patient-derived CLL cells. These findings establish that HR attenuation may be a therapeutically viable approach to selectively targeted treatment of cancers (and other pathologies) involving AID-expressing cells. Because AID mRNA expression is found in a high percentage of primary CLLs, as well as other cancers, this therapeutic concept has potential to benefit a large number of patients.

Although CLL is manageable in many cases, up to half of CLL patients will require therapy at some point in their disease course (Yee and O'Brien, 2006; Zent and Kay, 2011). Conventional first-line therapy for CLL involves treatment with purine analogues such as fludarabine with or without other agents, especially chlorambucil and/or rituximab (Dighiero and Hamblin, 2008). These combinations are reported to achieve complete remission in <40% of patients and usually for a duration of <3 yr before relapse with treatment refractory disease (Hallek, 2005). Major side effects of purine analogues like fludarabine include severe hematologic events such as profound neutropenia or fatal pancytopenia; life-threatening autoimmune reactions; serious, opportunistic infections; widespread neurological effects, including peripheral neuropathy; and induction of secondary tumors, especially of the skin (Cheson et al., 1999; Molica, 2005; Robak and Robak, 2007). Given that current chemotherapies for CLL and other indolent lymphoproliferative disorders are immunosuppressive and can cause devastating, long-term side effects without the promise of long-term durable remission, new treatment paradigms that target underlying mechanisms or disease-specific features are a clinical oncology imperative (Hallek, 2005; Yee and O'Brien, 2006; Dighiero and Hamblin, 2008). Though our data suggest that AID-mediated cytotoxicity could result in reduction of the post-GC B cell pool, and thus a mild, transient immunosuppression, we postulate that this would be more tolerable than the widespread suppression of adaptive and innate immunity after treatment with conventional chemotherapeutics such as fludarabine. Future testing in preclinical models is needed to examine this paradigm.

Accumulating evidence has implicated AID as a functionally significant mutator enzyme in a range of human cancers, including CLL (Kou et al., 2007; Klemm et al., 2009; Palacios et al., 2010; Shimizu et al., 2012). Aberrant AID activity leads to point mutations or DSBs in cellular proto-oncogenes or tumor suppressor genes that can drive tumor formation (Okazaki et al., 2003). The underlying cause of aberrant activation of AID in
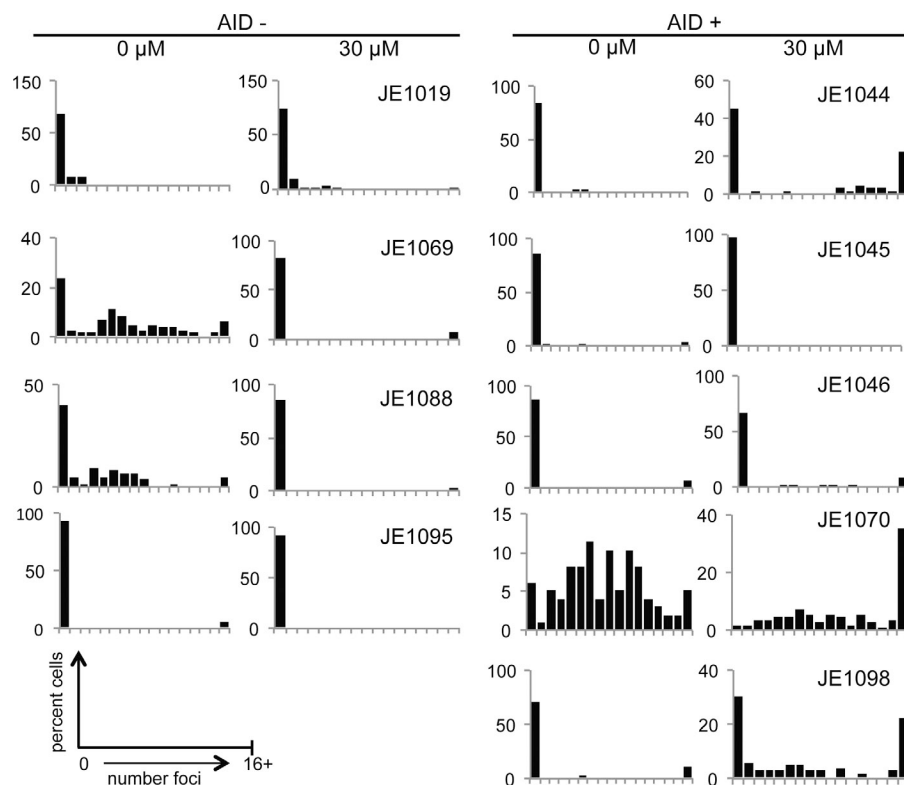
Figure 8. γ–H2AX foci distributions for CLLs cultured with 30 µM DIDS. CD5⁺ CD19⁺ sorted cells from primary CLL patient PBMC samples were cultured in media with 0 or 30 µM DIDS for 2 d before fixation on coverslips and immunostaining for phosphorylated γ-H2AX. Approximately 100 cells were counted for each sample. Foci distributions for AID⁻ CLLs (left) and AID⁺ CLLs (right) are represented as the percentage of cells (y axis) with the number of γ-H2AX foci plotted on the x axis. CLL tumor IDs are provided next to their individual distributions.

tumor cells is not yet understood, but some evidence suggests that persistent inflammatory signaling, perhaps caused by infection (Matsumoto et al., 2007) or other stimuli (Morita et al., 2011), can contribute to ectopic AID expression (Mechtcheriakova et al., 2012; Shimizu et al., 2012). We speculate that in normal cells and untreated tumor cells, efficient DNA repair systems mitigate the majority of AID-induced damage, allowing cellular survival while permitting accumulation of mutations over numerous cell divisions. Our data now indicate that inhibition of HR via DIDS treatment renders aberrant AID activity cytotoxic, owing to intolerable levels of unrepaired chromosomal breakage. Thus, AID expression may be converted from a proneoplastic role to an antineoplastic one by DNA repair inhibition.

As a putative treatment modality for AID-expressing malignancies, RAD51 inhibition is somewhat similar to, but conceptually distinct from, synthetic lethal strategies based on PARP inhibition. Synthetic lethality is defined genetically as an interaction in which two (or more) mutations that are individually tolerable result in cell lethality when combined. Clinically, this can be exploited for therapy when underlying mutations, such as BRCA1 or BRCA2 deficiency, render cancer cells susceptible to inhibition of additional pathways, such as PARP-mediated single-strand break repair, inducing conditional synthetic lethality selectively in the aberrant cells (Ashworth, 2008). In BRCA1- or BRCA2-deficient breast and ovarian cancer, PARP inhibition results in loss of both DSB and single-strand break repair, preventing repair of replication-associated DNA lesions, culminating in cell cycle arrest or death. In contrast, the approach described here exploits the concept of synergistic toxicity, defined as an interaction in which a mutation in one pathway renders the activity of a second pathway (either of which is individually tolerable) acutely damaging when combined. Whereas PARP-based synthetic lethality aims to minimize DNA repair efficiency leading to proliferation failure, our modality aims to maximize recombinase–mediated DNA damage leading to direct cytotoxicity. As such, these represent fundamentally distinct but possibly complementary therapeutic paradigms.

Here we begin to elucidate the mechanism of a new therapeutic concept. We show that DIDS inhibits RAD51, and by extension HR, which sensitizes cells to AID-generated DSBs, leading to cell death. Whether DIDS inhibits RAD51 through preventing complex formation or nuclear localization is not understood. In this context, RAD51 lacks a known nuclear localization sequence (NLS) and is thought to be imported into the nucleus via interactions with other NLS-containing proteins (Gildemeister et al., 2009). Thus, cytoplasmic accumulation of RAD51 caused by DIDS is likely a result of disrupted binding of RAD51 to one or more NLS-containing cofactors (Davies et al., 2001; Tarsounas et al., 2004; Thorslund et al., 2010). Furthermore, AID-generated genomic deoxyuridines are processed by UNG, culminating in CSR initiation to DSBs (Schrader et al., 2005). However, our data suggest that UNG is dispensable for the AID-dependent antileukemic effect triggered by DIDS treatment, as $Ung1^{-/-}$ cells respond as WT to DIDS treatment (Fig. 6 D). This result is not surprising as UNG has been demonstrated to be
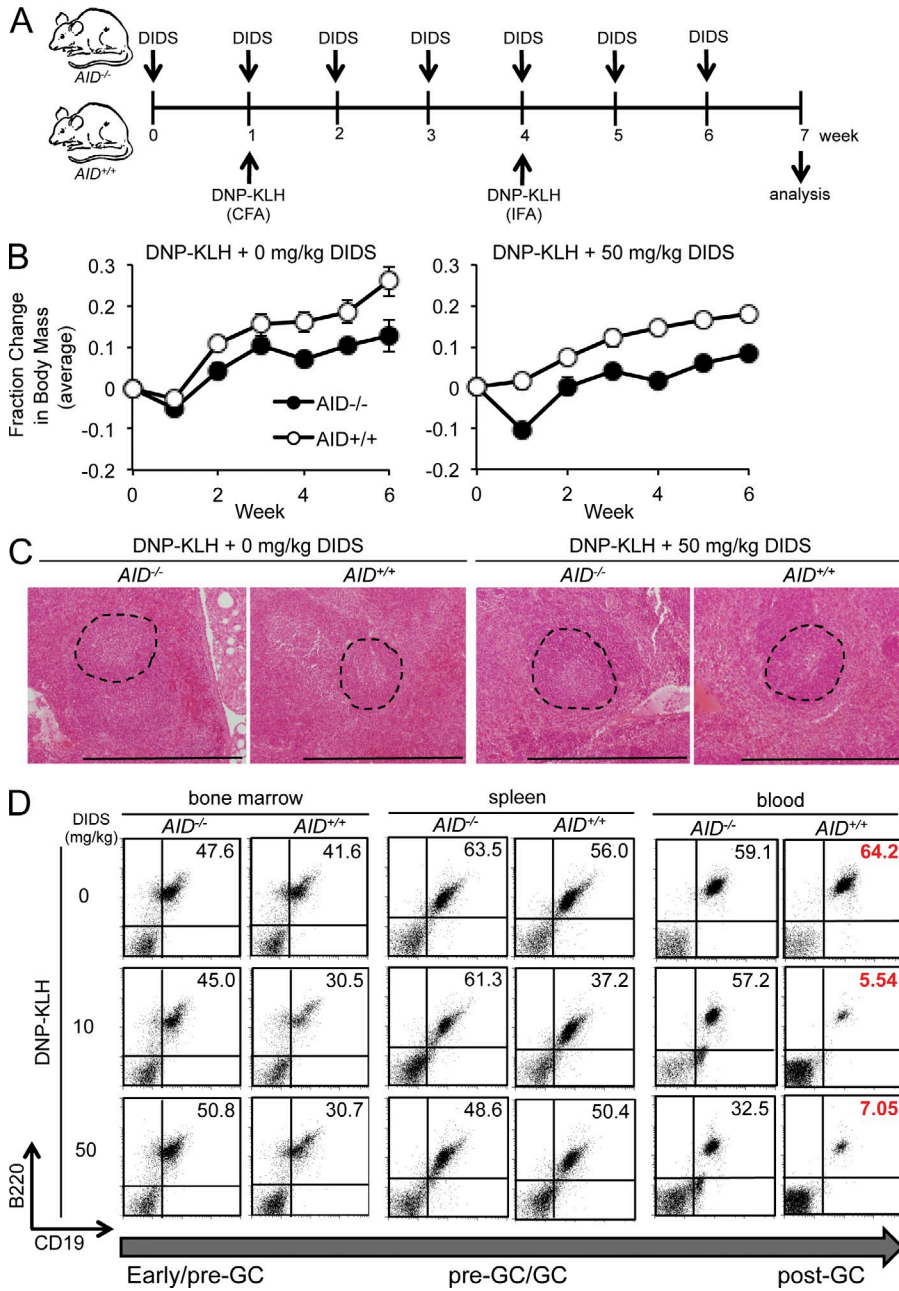
Figure 9. DIDS–induced ablation of circulating B lymphocytes in vivo requires AID. (A) Schematic of experimental design to examine the effect of systemic DIDS treatment in a primary mouse model. 8-wk-old *AID*−/− and *AID*+/+ mice were injected intraperitoneally with 0, 10, or 50 mg/kg DIDS weekly (*n* = 5 mice in each group). To activate AID, mice were immunized with DNP-KLH (with CFA) after 1 wk and given a booster treatment with DNP-KLH (with incomplete Freund's adjuvant [IFA]) after 4 wk. Mice were euthanized after 7 wk and analyzed. (B) Fraction change in body mass of mice treated with DNP-KLH and either 0 mg/kg (left) or 50 mg/kg (right) DIDS. Data represent the mean fractional change in body mass for five animals; error bars denote SEM. (C) H&E staining of *AID*+/+ and *AID*−/− spleens at necropsy. GCs are outlined by superimposed dashed lines. Bars, 500 μm. (D) Endpoint flow cytometry dot plot analysis of bone marrow, spleen, and peripheral blood from *AID*−/− and *AID*+/+ mice immunized with DNP-KLH and treated with 0, 10, or 50 mg/kg DIDS. Plots represent the population of cells in the lymphocyte gate stained for expression of B220 (y axis) and CD19 (x axis). The numbers in top right corner of each plot provide the percentage of B220+ CD19+ cells for each analysis. The progression of B cell maturation from early/pre-GC to post-GC is indicated below.

dispensable for the DNA cleavage step (Begum et al., 2007). Therefore, DSBs in collateral damage may require other glycosylases to form.

In summary, we have now established that small molecule inhibition of RAD51-mediated DSB repair sensitizes both primary and leukemic B cells to AID–initiated DSBs, culminating in growth suppression and apoptotic cell death. This suggests that pharmacologic attenuation of RAD51, and possibly other key HR factors, could be a useful therapeutic strategy to target AID-expressing tumors. Although our proof of principle experiments have focused on AID-expressing human CLL, AID expression has been noted in a wide range of other tumor types, including myeloid leukemias and a host of solid tumors. In this context, targeting HR in AID-positive acute myeloid leukemia may be especially promising, as AID has been implicated in aggressive disease associated with therapy resistance.

MATERIALS AND METHODS

Cell lines and cell culture. CH12-F3 cells were a gift from T. Honjo (Kyoto University, Kyoto, Japan). CH12-F3 cells were maintained in RPMI media with L-glutamine (Gibco), supplemented with 10% heat-inactivated FBS (Omega Scientific) and 5% NCTC 109 media (Gibco). CCRF-SB cells were purchased from the American Type Culture Collection and cultured according to manufacturer recommendations. Primary mouse splenocytes were obtained from 8–12-wk-old $AID^{-/-}$ or C57BL6/J mice and then either directly cultured or enriched for B220$^+$ IgM$^+$ B cells through depletion of CD43$^+$ cells via magnetic bead cell sorting (MACS; Miltenyi Biotec). Total splenocytes or purified B cells were maintained in RPMI medium containing L-glutamine and supplemented with 10% heat-inactivated FBS (Atlanta Biologicals). Cells were induced to activate AID and initiate Ig class switching as previously described (Hasham et al., 2010). Cell viability was determined through 0.2% Trypan blue (Lonza) staining and counting of dye-excluding (live) cells via a hemocytometer (Neubauer).

DR-GFP assay. The I-SceI expression vector pCBASce or a control vector pCAGGS (25 μg for U2OS DR-GFP cells and 40 μg for mES DR-GFP cells) was added to $5 × 10^6$ cells in 800 μl Opti-MEM in a 0.4-cm gap cuvette and electroporated by pulsing at 250 V, 950 μF. After electroporation, cells were placed in a 10-cm tissue culture dish with tissue culture media in the absence or presence of DIDS (30 μM for U2OS DR-GFP cells and 150 μM for mES DR-GFP cells). After 48 h, GFP$^+$ cells were quantified by flow cytometry using a FACScan (BD).

CLL tumor specimens. Before sample collection, patients consented according to HIPAA (Health Insurance Portability and Accountability Act of 1996) standards by individuals at CancerCare of Maine and the Maine Center for Cancer Medicine (Institutional Review Board Protocol #HS11-01). Patients were approached to be a part of this study as they came in for routine blood work or treatment and were considered eligible if they have ever had a prior diagnosis of CLL, regardless of treatment status. 8–16-ml blood samples from patients were collected via peripheral bleed into Vacutainer CPT tubes (BD), centrifuged to sequester red blood cells below the separation gel according to manufacturer instructions, and transported within 24 h to the Jackson Laboratory. Upon receipt, PBMCs were isolated from samples according to manufacturer specifications. Approximately $2 × 10^7$ cells were used for RNA preparation (below), and any remaining PBMCs were resuspended in RPMI media containing 50% FCS at a concentration of $0.5–1 × 10^8$ cells/ml and frozen for long-term storage in liquid nitrogen.

Immunofluorescence microscopy. After culture, cells were incubated for 2 h on poly-L-lysine–coated coverslips. Cells were then fixed in a 3% NBF, 2% sucrose solution, washed in DPBS, and permeabilized in 0.1% Triton X-100. Cells were incubated with primary antibodies (γ-H2AX, 1:400 [Bethyl Laboratories, Inc.]; active caspase-3, 1:100 [Abcam]; and Rad51, 1:100 [Abcam]). Secondary antibodies were either goat anti–rabbit IgG-TRITC (1:1,000; Jackson ImmunoResearch Laboratories, Inc.) or goat anti–rabbit IgG–Alexa Fluor 488 (1:500; Life Technologies). Coverslips were mounted on slides and imaged as previously described (Caddle et al., 2008).

RT-PCR. Total RNA was prepared from $2 × 10^7$ CLL patient PBMCs according to the RNeasy kit (QIAGEN). 250 ng RNA from each sample was used in RT-PCR reactions using the One-Step RT-PCR kit (QIAGEN) according to the manufacturer's instructions. Primers for AID were hAID forward, 5′-TCCTTTTCACTGGACTTTGG-3′; and hAID reverse, 5′-GACTGAGGTTGGGGTTCC-3′. Primers for GAPDH were hGAPDH forward, 5′-GAGTCAACGGATTTGGTCGT-3′; and hGAPDH reverse, 5′-TTGATTTTGGAGGGATCTCG-3′. RT-PCR reactions were electrophoresed on a 1.5% agarose TAE gel and visualized and imaged on a Gel-Doc System (Bio-Rad Laboratories). Expected band sizes were 196 bp for AID and 238 bp for GAPDH.

Real-time qPCR. 500 ng of total RNA was reverse transcribed to cDNA according to the MessageSensor RT kit (Ambion). Real-time qPCR was performed using SYBR green PCR master mix (Applied Biosystems) according to the manufacturer's instructions on an ABI 7500 instrument (Applied Biosystems). AID and GAPDH primers were as described for RT-PCR. The fold change in expression levels was determined by a comparative C_T method using the formula $2^{-\Delta\Delta C_T}$, where C_T is the threshold cycle of amplification. All samples were analyzed in triplicate and normalized to internal GAPDH controls.

Ung1 genotyping. Primers were as follows: Ung forward, 5′-GTGAATGCAGGGCTCACTTAAGTC-3′; Ung R2, 5′-CAGTGCCTATAACTTCAGCTCC-3′; and Neo forward, 5′-GCCGGTCTTGTCGATCAGGATGATC-3′. Cycling parameters were as follows: 94°C for 3 min, 94°C for 45 s, 57°C for 1 min, and 72°C for 1 min for 30 cycles; 72°C for 10 min. Ung R2 is the common primer; Ung$^{+/+}$ yields a 493-bp band, Ung$^{-/-}$ yields 600 bp, and Ung$^{+/-}$ yields both.

Lentiviral transduction and shRNA. CCRF-SB cells were transduced with lentivirus containing shRNA constructs targeting AID, TRCN0000412426 (AIDKD26) and TRCN0000050347 (AIDKD47; Sigma-Aldrich), as previously described (Hasham et al., 2010).

DNP-KLH mouse immunizations. Mice were immunized and challenged with 100 μg DNP-KLH (EMD Millipore) as described previously (Christianson et al., 1997).

Online supplemental material. Table S1, included as a separate Excel file, shows clinical annotations of CLL patient samples. Online supplemental material is available at http://www.jem.org/cgi/content/full/jem.20121258/DC1.

REFERENCES

Ashworth, A. 2008. A synthetic lethal therapeutic approach: poly(ADP) ribose polymerase inhibitors for the treatment of cancers deficient in DNA double-strand break repair. *J. Clin. Oncol.* 26:3785–3790. http://dx.doi.org/10.1200/JCO.2008.16.0812

Begum, N.A., N. Izumi, M. Nishikori, H. Nagaoka, R. Shinkura, and T. Honjo. 2007. Requirement of non-canonical activity of uracil DNA glycosylase for class switch recombination. *J. Biol. Chem.* 282:731–742. http://dx.doi.org/10.1074/jbc.M607439200

Caddle, L.B., M.G. Hasham, W.H. Schott, B.-J. Shirley, and K.D. Mills. 2008. Homologous recombination is necessary for normal lymphocyte development. *Mol. Cell. Biol.* 28:2295–2303. http://dx.doi.org/10.1128/MCB.02139-07

Chaudhuri, J., M. Tian, C. Khuong, K. Chua, E. Pinaud, and F.W. Alt. 2003. Transcription-targeted DNA deamination by the AID antibody diversification enzyme. *Nature.* 422:726–730. http://dx.doi.org/10.1038/nature01574

Cheson, B.D., D.A. Vena, J. Barrett, and B. Freidlin. 1999. Second malignancies as a consequence of nucleoside analog therapy for chronic lymphoid leukemias. *J. Clin. Oncol.* 17:2454–2460.

Christianson, G.J., W. Brooks, S. Vekasi, E.A. Manolfi, J. Niles, S.L. Roopenian, J.B. Roths, R. Rothlein, and D.C. Roopenian. 1997. Beta 2-microglobulin-deficient mice are protected from hypergammaglobulinemia and have defective antibody responses because of increased IgG catabolism. *J. Immunol.* 159:4781–4792.

Daboussi, F., A. Dumay, F. Delacôte, and B.S. Lopez. 2002. DNA double-strand break repair signalling: the case of RAD51 post-translational regulation. *Cell. Signal.* 14:969–975. http://dx.doi.org/10.1016/S0898-6568(02)00052-9

Davies, A.A., J.-Y. Masson, M.J. McIlwraith, A.Z. Stasiak, A. Stasiak, A.R. Venkitaraman, and S.C. West. 2001. Role of BRCA2 in control of the RAD51 recombination and DNA repair protein. *Mol. Cell.* 7:273–282. http://dx.doi.org/10.1016/S1097-2765(01)00175-7

Deans, B., C.S. Griffin, M. Maconochie, and J. Thacker. 2000. Xrcc2 is required for genetic stability, embryonic neurogenesis and viability in mice. *EMBO J.* 19:6675–6685. http://dx.doi.org/10.1093/emboj/19.24.6675

Deans, B., C.S. Griffin, P. O'Regan, M. Jasin, and J. Thacker. 2003. Homologous recombination deficiency leads to profound genetic instability in cells derived from Xrcc2-knockout mice. *Cancer Res.* 63:8181–8187.

Dighiero, G., and T.J. Hamblin. 2008. Chronic lymphocytic leukaemia. *Lancet.* 371:1017–1029. http://dx.doi.org/10.1016/S0140-6736(08)60456-0

Gildemeister, O.S., J.M. Sage, and K.L. Knight. 2009. Cellular redistribution of Rad51 in response to DNA damage: novel role for Rad51C. *J. Biol. Chem.* 284:31945–31952. http://dx.doi.org/10.1074/jbc.M109.024646

Hallek, M.; German CLL Study Group. 2005. Chronic lymphocytic leukemia (CLL): first-line treatment. *Hematology (Am Soc Hematol Educ Program).* 2005:285–291. http://dx.doi.org/10.1182/asheducation-2005.1.285

Hancer, V.S., M. Kose, R. Diz-Kucukkaya, A.S. Yavuz, and M. Aktan. 2011. Activation-induced cytidine deaminase mRNA levels in chronic lymphocytic leukemia. *Leuk. Lymphoma.* 52:79–84. http://dx.doi.org/10.3109/10428194.2010.531410

Hasham, M.G., N.M. Donghia, E. Coffey, J. Maynard, K.J. Snow, J. Ames, R.Y. Wilpan, Y. He, B.L. King, and K.D. Mills. 2010. Widespread genomic breaks generated by activation-induced cytidine deaminase are prevented by homologous recombination. *Nat. Immunol.* 11:820–826. http://dx.doi.org/10.1038/ni.1909

Hasham, M.G., K.J. Snow, N.M. Donghia, J.A. Branca, M.D. Lessard, J. Stavnezer, L.S. Shopland, and K.D. Mills. 2012. Activation-induced cytidine deaminase-initiated off-target DNA breaks are detected and resolved during S phase. *J. Immunol.* 189:2374–2382. http://dx.doi.org/10.4049/jimmunol.1200414

Heintel, D., E. Kroemer, D. Kienle, I. Schwarzinger, A. Gleiss, J. Schwarzmeier, R. Marculescu, T. Le, C. Mannhalter, A. Gaiger, et al; German CLL Study Group. 2004. High expression of activation-induced cytidine deaminase (AID) mRNA is associated with unmutated IGVH gene status and unfavourable cytogenetic aberrations in patients with chronic lymphocytic leukaemia. *Leukemia.* 18:756–762. http://dx.doi.org/10.1038/sj.leu.2403294

Ishida, T., Y. Takizawa, T. Kainuma, J. Inoue, T. Mikawa, T. Shibata, H. Suzuki, S. Tashiro, and H. Kurumizaka. 2009. DIDS, a chemical compound that inhibits RAD51-mediated homologous pairing and strand exchange. *Nucleic Acids Res.* 37:3367–3376. http://dx.doi.org/10.1093/nar/gkp200

Kawabata, M., T. Kawabata, and M. Nishibori. 2005. Role of recA/RAD51 family proteins in mammals. *Acta Med. Okayama.* 59:1–9.

Klemm, L., C. Duy, I. Iacobucci, S. Kuchen, G. von Levetzow, N. Feldhahn, N. Henke, Z. Li, T.K. Hoffmann, Y.M. Kim, et al. 2009. The B cell mutator AID promotes B lymphoid blast crisis and drug resistance in chronic myeloid leukemia. *Cancer Cell.* 16:232–245. http://dx.doi.org/10.1016/j.ccr.2009.07.030

Kou, T., H. Marusawa, K. Kinoshita, Y. Endo, I.M. Okazaki, Y. Ueda, Y. Kodama, H. Haga, I. Ikai, and T. Chiba. 2007. Expression of activation-induced cytidine deaminase in human hepatocytes during hepatocarcinogenesis. *Int. J. Cancer.* 120:469–476. http://dx.doi.org/10.1002/ijc.22292

Liu, Z., X. Wu, Y. Duan, Y. Wang, B. Shan, J. Kong, X. Ma, and Y. Bao. 2011. AID expression is correlated with Bcr-Abl expression in CML-LBC and can be down-regulated by As2O3 and/or imatinib. *Leuk. Res.* 35:1355–1359. http://dx.doi.org/10.1016/j.leukres.2011.04.020

Matsumoto, Y., H. Marusawa, K. Kinoshita, Y. Endo, T. Kou, T. Morisawa, T. Azuma, I.-M. Okazaki, T. Honjo, and T. Chiba. 2007. *Helicobacter pylori* infection triggers aberrant expression of activation-induced cytidine deaminase in gastric epithelium. *Nat. Med.* 13:470–476. http://dx.doi.org/10.1038/nm1566

McBride, K.M., A. Gazumyan, E.M. Woo, V.M. Barreto, D.F. Robbiani, B.T. Chait, and M.C. Nussenzweig. 2006. Regulation of hypermutation by activation-induced cytidine deaminase phosphorylation. *Proc. Natl. Acad. Sci. USA.* 103:8798–8803. http://dx.doi.org/10.1073/pnas.0603272103

Mechtcheriakova, D., M. Svoboda, A. Meshcheryakova, and E. Jensen-Jarolim. 2012. Activation-induced cytidine deaminase (AID) linking immunity, chronic inflammation, and cancer. *Cancer Immunol. Immunother.* 61:1591–1598. http://dx.doi.org/10.1007/s00262-012-1255-z

Molica, S. 2005. Second neoplasms in chronic lymphocytic leukemia: incidence and pathogenesis with emphasis on the role of different therapies. *Leuk. Lymphoma.* 46:49–54. http://dx.doi.org/10.1080/10428190400007524

Morita, S., Y. Matsumoto, S. Okuyama, K. Ono, Y. Kitamura, A. Tomori, T. Oyama, Y. Amano, Y. Kinoshita, T. Chiba, and H. Marusawa. 2011. Bile acid-induced expression of activation-induced cytidine deaminase during the development of Barrett's oesophageal adenocarcinoma. *Carcinogenesis.* 32:1706–1712. http://dx.doi.org/10.1093/carcin/bgr194

Moynahan, M.E., and M. Jasin. 2010. Mitotic homologous recombination maintains genomic stability and suppresses tumorigenesis. *Nat. Rev. Mol. Cell Biol.* 11:196–207. http://dx.doi.org/10.1038/nrm2851

Moynahan, M.E., A.J. Pierce, and M. Jasin. 2001. BRCA2 is required for homology-directed repair of chromosomal breaks. *Mol. Cell.* 7:263–272. http://dx.doi.org/10.1016/S1097-2765(01)00174-5

Muramatsu, M., K. Kinoshita, S. Fagarasan, S. Yamada, Y. Shinkai, and T. Honjo. 2000. Class switch recombination and hypermutation require activation-induced cytidine deaminase (AID), a potential RNA editing enzyme. *Cell.* 102:553–563. http://dx.doi.org/10.1016/S0092-8674(00)00078-7

Nakanishi, K., Y.G. Yang, A.J. Pierce, T. Taniguchi, M. Digweed, A.D. D'Andrea, Z.Q. Wang, and M. Jasin. 2005. Human Fanconi anemia monoubiquitination pathway promotes homologous DNA repair. *Proc. Natl. Acad. Sci. USA.* 102:1110–1115. http://dx.doi.org/10.1073/pnas.0407796102

Okazaki, I.M., H. Hiai, N. Kakazu, S. Yamada, M. Muramatsu, K. Kinoshita, and T. Honjo. 2003. Constitutive expression of AID leads to tumorigenesis. *J. Exp. Med.* 197:1173–1181. http://dx.doi.org/10.1084/jem.20030275

Palacios, F., P. Moreno, P. Morande, C. Abreu, A. Correa, V. Porro, A.I. Landoni, R. Gabus, M. Giordano, G. Dighiero, et al. 2010. High expression of AID and active class switch recombination might account for a more aggressive disease in unmutated CLL patients: link with an activated microenvironment in CLL disease. *Blood.* 115:4488–4496. http://dx.doi.org/10.1182/blood-2009-12-257758

Pasqualucci, L., G. Bhagat, M. Jankovic, M. Compagno, P. Smith, M. Muramatsu, T. Honjo, H.C. Morse III, M.C. Nussenzweig, and R. Dalla-Favera. 2008. AID is required for germinal center-derived lymphomagenesis. *Nat. Genet.* 40:108–112. http://dx.doi.org/10.1038/ng.2007.35

Robak, E., and T. Robak. 2007. Skin lesions in chronic lymphocytic leukemia. *Leuk. Lymphoma.* 48:855–865. http://dx.doi.org/10.1080/10428190601137336

Robbiani, D.F., S. Bunting, N. Feldhahn, A. Bothmer, J. Camps, S. Deroubaix, K.M. McBride, I.A. Klein, G. Stone, T.R. Eisenreich, et al. 2009. AID produces DNA double-strand breaks in non-Ig genes and mature B cell lymphomas with reciprocal chromosome translocations. *Mol. Cell.* 36:631–641. http://dx.doi.org/10.1016/j.molcel.2009.11.007

Rogakou, E.P., D.R. Pilch, A.H. Orr, V.S. Ivanova, and W.M. Bonner. 1998. DNA double-stranded breaks induce histone H2AX phosphorylation on serine 139. *J. Biol. Chem.* 273:5858–5868. http://dx.doi.org/10.1074/jbc.273.10.5858

Sale, J.E., D.M. Calandrini, M. Takata, S. Takeda, and M.S. Neuberger. 2001. Ablation of XRCC2/3 transforms immunoglobulin V gene conversion into somatic hypermutation. *Nature.* 412:921–926. http://dx.doi.org/10.1038/35091100

Schrader, C.E., E.K. Linehan, S.N. Mochegova, R.T. Woodland, and J. Stavnezer. 2005. Inducible DNA breaks in Ig S regions are dependent on AID and UNG. *J. Exp. Med.* 202:561–568. http://dx.doi.org/10.1084/jem.20050872

Shimizu, T., H. Marusawa, Y. Endo, and T. Chiba. 2012. Inflammation-mediated genomic instability: roles of activation-induced cytidine

deaminase in carcinogenesis. *Cancer Sci.* 103:1201–1206. http://dx.doi .org/10.1111/j.1349-7006.2012.02293.x

Shinmura, K., H. Igarashi, M. Goto, H. Tao, H. Yamada, S. Matsuura, M. Tajima, T. Matsuda, A. Yamane, K. Funai, et al. 2011. Aberrant expression and mutation–inducing activity of AID in human lung cancer. *Ann. Surg. Oncol.* 18:2084–2092. http://dx.doi.org/10.1245/s10434-011-1568-8

Shinohara, A., H. Ogawa, and T. Ogawa. 1992. Rad51 protein involved in repair and recombination in S. cerevisiae is a RecA-like protein. *Cell.* 69:457–470. http://dx.doi.org/10.1016/0092-8674(92)90447-K

Staszewski, O., R.E. Baker, A.J. Ucher, R. Martier, J. Stavnezer, and J.E.J. Guikema. 2011. Activation-induced cytidine deaminase induces reproducible DNA breaks at many non-Ig Loci in activated B cells. *Mol. Cell.* 41:232–242. http://dx.doi.org/10.1016/j.molcel.2011.01.007

Steurer, M., G. Pall, S. Richards, G. Schwarzer, J. Bohlius, and R. Greil; Cochrane Haematologic Malignancies Group. 2006. Single-agent purine analogues for the treatment of chronic lymphocytic leukaemia: a systematic review and meta-analysis. *Cancer Treat. Rev.* 32:377–389. http://dx.doi .org/10.1016/j.ctrv.2006.05.002

Sung, P., and D.L. Robberson. 1995. DNA strand exchange mediated by a RAD51-ssDNA nucleoprotein filament with polarity opposite to that of RecA. *Cell.* 82:453–461. http://dx.doi.org/10.1016/0092-8674(95)90434-4

Suwaki, N., K. Klare, and M. Tarsounas. 2011. RAD51 paralogs: roles in DNA damage signalling, recombinational repair and tumorigenesis. *Semin. Cell Dev. Biol.* 22:898–905. http://dx.doi.org/10.1016/j.semcdb .2011.07.019

Tarsounas, M., A.A. Davies, and S.C. West. 2004. RAD51 localization and activation following DNA damage. *Philos. Trans. R. Soc. Lond. B Biol. Sci.* 359:87–93. http://dx.doi.org/10.1098/rstb.2003.1368

Thacker, J. 2005. The RAD51 gene family, genetic instability and cancer. *Cancer Lett.* 219:125–135. http://dx.doi.org/10.1016/j.canlet.2004.08.018

Thorslund, T., M.J. McIlwraith, S.A. Compton, S. Lekomtsev, M. Petronczki, J.D. Griffith, and S.C. West. 2010. The breast cancer tumor suppressor BRCA2 promotes the specific targeting of RAD51 to single-stranded DNA. *Nat. Struct. Mol. Biol.* 17:1263–1265. http://dx.doi.org/10.1038/ nsmb.1905

Vasconcelos, Y., F. Davi, V. Levy, P. Oppezzo, C. Magnac, A. Michel, M. Yamamoto, O. Pritsch, H. Merle-Béral, K. Maloum, et al. 2003. Binet's staging system and VH genes are independent but complementary prognostic indicators in chronic lymphocytic leukemia. *J. Clin. Oncol.* 21:3928–3932. http://dx.doi.org/10.1200/JCO.2003.02.134

Yee, K.W.L., and S.M. O'Brien. 2006. Chronic lymphocytic leukemia: diagnosis and treatment. *Mayo Clin. Proc.* 81:1105–1129. http://dx.doi.org/ 10.4065/81.8.1105

Zan, H., and P. Casali. 2008. AID- and Ung-dependent generation of staggered double-strand DNA breaks in immunoglobulin class switch DNA recombination: a post-cleavage role for AID. *Mol. Immunol.* 46:45–61. http://dx.doi.org/10.1016/j.molimm.2008.07.003

Zent, C.S., and N.E. Kay. 2011. Management of patients with chronic lymphocytic leukemia with a high risk of adverse outcome: the Mayo Clinic approach. *Leuk. Lymphoma.* 52:1425–1434. http://dx.doi.org/ 10.3109/10428194.2011.568654